J. Mod. Power Syst. Clean Energy (2015) 3(2):212–220
DOI 10.1007/s40565-015-0123-1

CrossMark

Energy management with dual droop plus frequency dividing coordinated control strategy for electric vehicle applications

Wuhua LI (✉), Chi XU, Hongbin YU, Yunjie GU, Xiangning HE

MPCE

Abstract In this paper, a dual droop-frequency diving coordinated control strategy is proposed for electric vehicle (EV) applications, where the hybrid energy storage system (HESS) with supercapacitors and batteries is integrated to prolong the life time of storage elements. The dynamic power allocation between the supercapacitor and batteries are obtained through the voltage cascaded control, upon which the high and low frequency power fluctuation are absorbed by the supercapacitors and batteries respectively to fully exploit the advantages of the supercapacitors and batteries. Moreover, the power capacity is scaled up by connecting storage blocks in parallel. A dual droop control scheme for parallel-connected energy storage system and its operation principle is introduced on the aspect of current sharing characteristic and state-of-charging (SOC) management. After detailed analysis and formula derivation, the corresponding loop parameters are designed. Through this control method, the current sharing performance is ensured and each block makes the self-adaptive adjustment according to their SOC. Consequently, the load power can be shared effectively, which helps to avoid the over-charge/over-discharge operation and contributes to the life cycle of the energy storage system. Each module is autonomous controlled without the necessity of communication, which is easy, economic and effective to realize. Finally, the simulation and experimental results are exhibited to verify the effectiveness of the proposed control scheme.

Keywords Dual droop control, Frequency diving coordinated control, Hybrid energy storage system, Electric vehicle

1 Introduction

The energy storage system (ESS) plays a key role in deciding the electric vehicle's performance and reliability [1–3]. Compared with the energy storage system solely structured by only batteries or supercapacitors, a hybrid energy storage system comprising both high power density and high energy density storage units, gains better performance, such as high power rating, high energy capacity, short response time, and extended the life cycle of the ESS [4–7]. Control, robustness, stability, efficiency, and optimization of HESS remain an essential research area [8]. How to reinforce the complementary advantages of batteries and supercapacitors, the current sharing and SOC management of battery are key issues that need to be considered [9–12].

Many studies have been done upon the dynamic power sharing between batteries and supercapacitors [13–15]. The main control objective is to achieve the dynamic allocation of high frequency power demands and low frequency power demands to the batteries and supercapacitors respectively. In [14], a piecewise linear relationship between the current of the battery and supercapacitor decides the power distribution. When the load power varies tremendously, the current of supercapacitor increases dramatically. As a result, the fluctuating power is mainly compensated by the supercapacitor with fast response. However, in the case of small variation of the load power, all the power is balanced by the battery, which leads to frequent charge and discharge cycles. This may do great harm to the battery and shorten its service life. To separate the responses in frequency between these two energy

CrossCheck date: 27 February 2015

Received: 11 November 2014 / Accepted: 10 April 2015 / Published online: 14 May 2015

W. LI, C. XU, H. YU, Y. GU, X. HE, Zhejiang University, Hangzhou 310027, China
(✉) e-mail: woohualee@zju.edu.cn

storages, the power demand are divided into low frequency and high frequency components in [15]. And through the bus and supercapacitor voltage cascaded control, the converter current references are set such that the low frequency component is supplied by the battery and the high frequency component is supplied by the supercapacitor [16]. However, only one battery and one supercapacitor are concerned, which limits its applications in the high power occasion.

In [16–21], the total current demand is derived from the difference between the energy source and load power. Then the low-frequency component of the current, namely the total current reference for the battery interfacing power converters, is generated by passing this current reference through a low-pass filter (LPF), while the rest of the current is the reference for supercapacitors. However, the calculation of the total current demand requires the information of all energy source and load power. It relies on a wide communication bandwidth with the increasing number of interfaces, which decreases the system reliability. Meanwhile, the average current control is adopted for current sharing. Such centralized energy management system relies heavily upon the energy control center itself, resulting in inadequate system reliability and scalability, which is not suitable for systems with dynamic structure.

On the other hand, the batteries have the operation limitations in practice. Without a proper battery management, it may come into being serious problems, such as the over-charging, over-discharging, imbalance of voltage among the cells. Therefore, it is a necessity to develop advanced control strategies for the battery equalization. In [16, 18–22], SOC is taken into account in energy control center with centralized control, whose drawback is the less flexible and not appropriate in an expandable system. An attenuation coefficient, with consideration of factors like battery terminal voltage and SOC, is multiplied by the battery current reference in the control loop to guarantee the efficient and safe operation of batteries in [23]. However, the current reference restriction that no power outputs once the battery voltage exceeds the bounds is too rigorous.

Combined with advantages of the conventional droop control, which features high expandability and reliability, the dual droop frequency dividing coordinated control is derived for HESS in this paper with consideration of power sharing between batteries and supercapacitors and SOC of batteries. By employing this control scheme, the dynamic power sharing between two energy storage mediums is ensured with the DC bus and supercapacitor voltage cascaded control. While dual droop control, as an extension of the conventional droop control, realizes the current sharing and SOC management of different power modules without requirement of communication, which increases the system reliability and flexibility.

2 Proposed control strategy for HESS

Figure 1 shows an electric vehicle propulsion system with HESS, which contains both high energy density and high power density storage elements. The battery packs, which provide power during the intermittent of the renewable energy sources, are connected to the DC bus by modular bi-directional DC-DC converters for the convenience of battery capacity expansion. While the supercapacitors are connected to the DC bus by multiple converters because of the high power rating.

The detailed control block of HESS is depicted in Fig. 2. C_{Bus} is the bus capacitor, and the power fluctuation caused by the motor drive is presented by a current source i_{bus}. For controlling the bi-directional DC/DC converters (BDCs), a cascaded control scheme using the inner current-control loop and outer voltage-control loop is realized, where i_{L_ref} is the current reference and the current transfer function is defined as $G_{BDC}(s)$. i_{Bat}, i_{SC} are the currents of the batteries and supercapacitors, respectively. i_{Bus_Bat}, i_{Bus_SC} are the corresponding current into the DC bus. $G_{vcSC}(s)$, H_{vBus}, V_{Bus_ref} are the compensators, feedback coefficient and voltage reference of the DC bus voltage control loop. The corresponding definitions of supercapacitor voltage control loop are expressed as $G_{vcBat}(s)$, H_{vSC}, V_{SC_ref}. And V_{Bus}, V_{SC}, V_{Bat} are the voltage of DC Bus, supercapacitor and battery. The conventional droop control is employed to realize the current sharing among the BDCs for supercapacitor, and the dual droop control is adopted for the current sharing and SOC management of the batteries. The frequency diving control method is realized through the DC bus and supercapacitor voltage cascaded control.

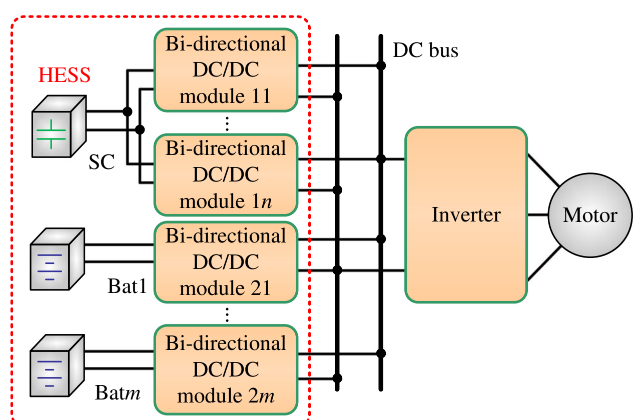

Fig. 1 Modular hybrid energy storage propulsion system

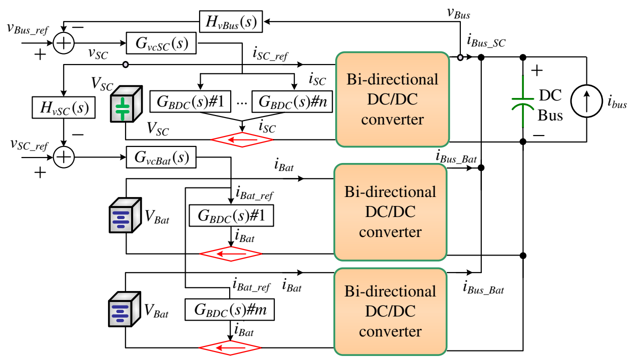

Fig. 2 Modular hybrid energy storage propulsion system

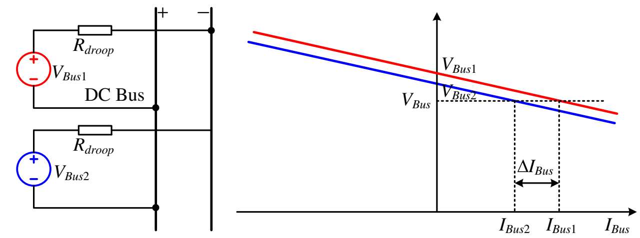

Fig. 3 Parallel operation of power converters with droop control and droop curves

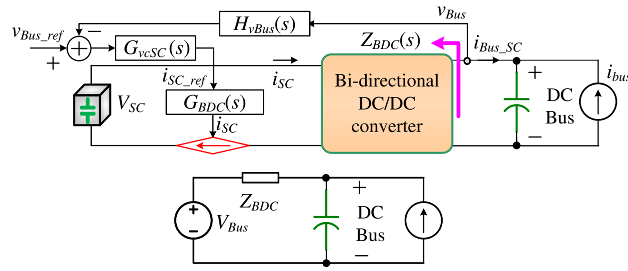

Fig. 4 Control scheme for supercapacitor converter

Table 1 Parameters of HESS

Components	Parameters
DC bus voltage feedback coefficient ($H_{vBus}(s)$)	8.533
Supercapacitor voltage feedback coefficient ($H_{vSC}(s)$)	100
DC Bus Capacitor (C_{Bus})	3000 μF
Supercapacitor capacity (C_{SC})	130 F
ESR of supercapacitor (R_{SC})	8m Ω
Supercapacitor voltage range (V_{SC})	30–60 V
Battery capacity	15 A h
Battery voltage range (V_{Bat})	40–56 V
DC bus voltage (V_{Bus})	400 V
Current transfer function gain ($G_{BDC}(s)$)	0.0444
Bandwidth of current control loop	400 Hz
Modular converter power (P_{out})	1500 W

To analyze and verify the effectiveness of the control strategy, a HESS, with the combination of batteries and supercapacitor, is built with parameters listed in Table 1.

2.1 Control design of power modules for supercapacitor

A DC-DC converter with droop controller can be simplified as an electric circuit with an ideal DC voltage source in series with an output resistance, as in Fig. 3. One promising way to realize droop control is by setting the virtual output impedance R_{droop} of DC-DC converter. A schematic diagram of two parallel connected converter modules and the corresponding droop curves are depicted in Fig. 3. The difference of output currents ΔI_{Bus} can be derived as

$$\Delta I_{Bus} = \frac{V_{Bus1} - V_{Bus2}}{R_{droop}} \tag{1}$$

where V_{Bat1} and V_{Bat2} are the no-load voltage of each module.

As presented in [19], the input current reference i_{SC_ref} for the supercapacitor converter is used to regulate the output voltage (V_{Bus}) at the reference level. From Fig. 4, the virtual output impedance of the supercapacitor converter is obtained by

$$Z_{BDC}(s) = \frac{1}{H_{vBus}(s)G_{vcSC}(s)G_{BDC}(s)\frac{V_{SC}}{V_{Bus}}} \tag{2}$$

In order to realize the *V-I* droop curves as shown in Fig. 3, the compensator $G_{vcSC}(s)$ can be derived as

$$G_{vcSC}(s) = \frac{1}{H_{vBus}(s)G_{BDC}(s)\frac{V_{SC}}{V_{Bus}}}\frac{1}{R_{d\_SC}} \tag{3}$$

Hence the output impedance $Z_{BDC}(s)$ equals to R_{d_SC}.

Considering n converter modules in parallel, the open loop transfer function of DC bus voltage $G_{vBuspoc}(s)$ is n times of $G_{vBusoc}(s)$, which is given by

$$\begin{aligned} G_{vBuspoc}(s) &= nG_{vBusoc}(s) = nG_{vcSC}(s)G_{BDC}(s)\frac{V_{SC}}{V_{Bus}} \\ \frac{1}{C_{Bus}s}H_{vBus}(s) &= \frac{n}{R_{d\_SC}C_{Bus}s} \end{aligned} \tag{4}$$

From (4), the bandwidth of DC bus voltage loop is decided by the number of branches in parallel n and the droop coefficient R_{d_SC}. The bandwidth of DC bus voltage loop is set at 5 Hz with consideration of the supercapacitor response time (in milliseconds). In the case of two converter modules in parallel, the droop coefficient R_{d_SC} is 21.2 Ω. If the voltage difference between V_{Bat1} and V_{Bat2} after calibration is 0.2% of the output voltage, namely 1.6

V, the difference of output current ΔI_{Bus} can be obtained by (1), which is 0.075 A and 4% of current in full load case. So the effect in distributing current equally is satisfied.

The open and close loop transfer function after compensation $G_{vBuspoc}(s)$, $G_{vBuspc}(s)$ are obtained by (5) and (6), while the current transfer function from battery to supercapacitor $G_{iSC\_iBatp}(s)$ is given by (7).

$$G_{vBuspoc}(s) = \frac{z_{c\_Bus}}{s} \tag{5}$$

$$G_{vBuspc}(s) = \frac{G_{vBuspoc}(s)/H_{vBus}(s)}{1+G_{vBuspoc}(s)} \approx \frac{z_{c\_Bus}}{s+z_{c\_Bus}} \frac{1}{H_{vBus}(s)} \tag{6}$$

$$\begin{aligned} G_{i_{SC}\_i_{BatP}}(s) &= -G_{vBuspc}(s)H_{vBus}(s)\frac{V_{Bat}}{V_{SC}} \\ &\approx \frac{z_{c\_Bus}}{s+z_{c\_Bus}}\frac{V_{Bat}}{V_{SC}} \end{aligned} \tag{7}$$

where z_{c_Bus} equals to $n/(R_{d\_SC}C_{Bus})$.

2.2 Control design of power modules for batteries

The equation of droop control for batteries is listed as (8), where V_{SC0} is the no-load voltage of each module, R_{d_Bat} is the drop coefficient and I_{Bat} is the battery current. If all the battery converters are controlled under the same droop curve, the batteries with lower SOC will go into over discharge while those with higher SOC will be over charged, which significantly decrease the system reliability. In order to balance SOC of each battery unit, a dual droop control scheme is proposed by introducing battery SOC into droop control scheme, which is shown in Fig. 5.

$$V_{SC} = V_{SC0} - R_{d\_Bat}I_{Bat} \tag{8}$$

V_{SC0_1}, V_{SC0_2} are the supercapacitor voltage reference for each battery converter, which are decided with their SOCs as in (9)

$$V_{SC0} = V^*_{SC0} + k_{v\_SOC}SOC \tag{9}$$

where V^*_{SC0} is the supercapacitor voltage reference under the circumstance of the minimum SOC and k_{v_SOC} is the secondary droop coefficient.

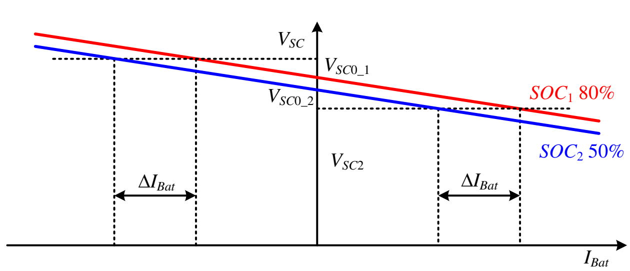

Fig. 5 Dual droop control scheme for battery converters

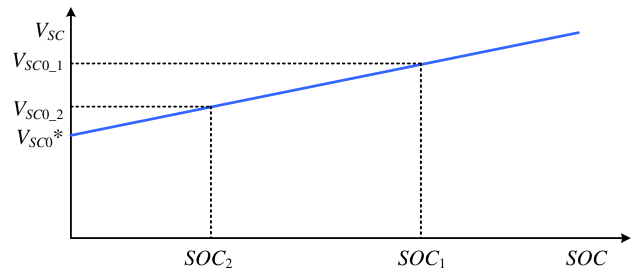

Fig. 6 Secondary droop between battery SOC and V^*_{SC0}

Equation (9) is drawn in Fig. 6, which achieves droop curves shifting up and down as presented in Fig. 5. Thus the battery with higher SOC takes in smaller current and gives out bigger current, which contributes to SOC balancing among the battery units.

The difference of battery currents ΔI_{Bat} is derived by

$$\Delta I_{Bat} = I_{Bat1} - I_{Bat2} = \frac{V_{SC0\_1} - V_{SC0\_2}}{R_{d\_Bat}} \tag{10}$$

$$\begin{aligned} V_{SC0\_1} - V_{SC0\_2} &= k_{v\_SOC}(SOC_1 - SOC_2) \\ &= k_{v\_SOC}\Delta SOC \end{aligned} \tag{11}$$

By substituting (11) into (12), ΔI_{Bat} is expressed as

$$\Delta I_{Bat} = \frac{k_{v\_SOC}\Delta SOC}{R_{d\_Bat}} \tag{12}$$

The battery SOC is related to its initial SOC, i.e. SOC_0 and the battery current as given by

$$SOC = SOC_0 - \frac{\int I_{Bat}\mathrm{d}t}{C_{Bat}} \tag{13}$$

So the difference of SOCs can be calculated as following

$$\begin{aligned} \Delta SOC &= SOC_1 - SOC_2 = SOC_{0_1} - SOC_{0_2} \\ &\quad - \frac{\int (I_{Bat1} - I_{Bat2})\mathrm{d}t}{C_{Bat}} = \Delta SOC_0 - \frac{\int \Delta I_{Bat}\mathrm{d}t}{C_{Bat}} \end{aligned} \tag{14}$$

Carrying out Laplace transform on (12) and (14), (15) and (16) can be derived

$$\Delta I_{Bat}(s) = \frac{k_{v\_SOC}\Delta SOC(s)}{R_{d\_Bat}} \tag{15}$$

$$\Delta SOC(s) = \Delta SOC_0 - \frac{\Delta I_{Bat}(s)}{C_{Bat}s} \tag{16}$$

By substituting (15) into (16), the difference of SOCs and battery currents are expressed as

$$\Delta SOC(s) = \frac{R_{d\_Bat}C_{Bat}s}{R_{d\_Bat}C_{Bat}s + k_{v\_SOC}}\Delta SOC_0 \tag{17}$$

$$\Delta I_{Bat}(s) = \frac{k_{v\_SOC}C_{Bat}s}{R_{d\_Bat}C_{Bat}s + k_{v\_SOC}}\Delta SOC_0 \tag{18}$$

According to (17), the SOC balance is a first order system so the difference of SOCs gradually deceases to zero with some decay time constant T_{SOC} as given in (19). Consequently the difference of battery currents turns to zero, realizing the SOC balancing as demonstrated in (18).

$$T_{SOC} = \frac{R_{d\_Bat} C_{Bat}}{k_{v\_SOC}} \tag{19}$$

3 Design considerations of proposed control strategy

3.1 Primary droop control parameter design

The block diagram of the supercapacitor voltage control loop is depicted in Fig. 7, where the supercapacitor is modeled as a capacitor C_{SC} and a resistor R_{SC} in series. And the impedance of the supercapacitor $Z_{SC}(s) = (R_{SC}C_{SC}s+1)/(C_{SC}s)$. The relationship between the supercapacitor voltage and the battery current can be derived by

$$v_{SC}(s) = \frac{v_{SC\_ref}}{H_{vSC}(s)} - \frac{1}{G_{vcBat}(s) G_{BDC}(s) H_{vSC}(s)} i_{Bat}(s) \tag{20}$$

In order to lower the gain around zero introduced by the supercapacitor impedance so as to suppress the batteries' response to the power fluctuation around the zero frequency, the compensator $G_{vcBat}(s)$ is designed as (20) where $z_{SC} = 1/(R_{SC}C_{SC})$ and the droop equation is derived by (22).

$$G_{vcBat}(s) = \frac{1}{H_{vSC}(s) G_{BDC}(s)} \frac{1}{R_{d\_Bat}} \frac{z_{SC}}{s + z_{SC}} \tag{21}$$

$$v_{SC}(s) = \frac{v_{SC\_ref}}{H_{vSC}(s)} - R_{d\_Bat} \frac{s + z_{SC}}{z_{SC}} i_{Bat}(s) \tag{22}$$

For the DC component, namely $s = 0$, the droop equation is simplified as following

$$v_{SC}(0) = \frac{v_{SC\_ref}}{H_{vSC}(0)} - R_{d\_Bat} i_{Bat}(0) \tag{23}$$

The bandwidth of the supercapacitor voltage loop is set at 0.05 Hz considering the batteries response time (in seconds). In the case of two converter modules in parallel, the droop coefficient R_{d_SC} is 0.05 Ω.

3.2 Secondary droop control parameter design

The secondary droop control between the supercapacitor voltage reference and SOC is achieved by adding a feedforward loop into the supercapacitor voltage control loop, as presented in Fig. 8. The secondary droop equation in steady state is given by

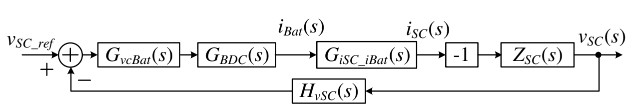

Fig. 7 Block diagram of supercapacitor voltage control loop

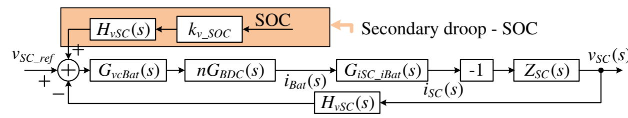

Fig. 8 Block diagram of dual droop control for battery units

$$V_{SC} = \frac{v_{SC\_ref}}{H_{vSC}} + k_{v\_SOC} SOC \tag{24}$$

In order not to influence the stability of the supercapacitor voltage control loop, the SOC balancing time constant T_{SOC} is set as 300 s, far larger than the corresponding time of the cross-over frequency in the supercapacitor voltage control loop (20 s). From (19), the secondary droop coefficient k_{v_SOC} can be obtained.

3.3 System response to power fluctuation

The relationship between the control parameters and frequency response range is analyzed to theoretically verify the proposed control strategy.

The transfer block diagram of response of the supercapacitor current and battery current to power fluctuation is plotted in Fig. 9.

The transfer function from the supercapacitor current to the battery current is obtained by

$$\begin{aligned} G_{i_{Bat}\_i_{SCP}}(s) &= Z_{SC}(s) H_{vSC}(s) n G_{vcBat}(s) G_{BDC}(s) \\ &= \frac{z_{c\_SC}}{s} \frac{V_{SC}}{V_{Bat}} \end{aligned} \tag{25}$$

where z_{c_SC} is the crossover frequency of supercapacitor voltage control loop.

From Fig. 9, the output impedance of HESS can be calculated by

$$Z_{op}(s) = \frac{v_{Bus}(s)}{i_{bus}(s)} = \frac{1}{1 + G_{vBuspoc}(s)(1 + G_{i_{Bat}\_i_{SCP}}(s) \frac{V_{Bat}}{V_{SC}})}$$
$$\frac{1}{C_{Bus}s} = \frac{s}{(s + z_{c\_SC})(s + z_{c\_Bus}) C_{Bus}} \tag{26}$$

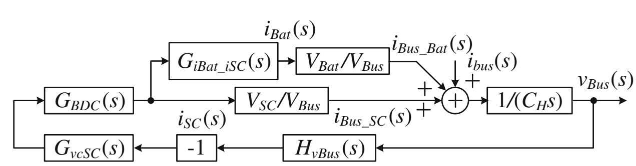

Fig. 9 Transfer block diagram of response of supercapacitor current and battery current to power fluctuation

Therefore, the transfer function of the DC bus capacitor current, supercapacitor current and batteries current to power fluctuation $G_{iCBus\_ibusp}(s)$, $G_{iBus\_SC\_ibusp}(s)$ and $G_{iBus\_Bat\_ibusp}(s)$ can be derived by

$$G_{i_{CBus}\_i_{busP}}(s) = \frac{Z_{op}(s)}{\frac{1}{C_{Bus}s}} = \frac{s^2}{(s+z_{c\_SC})(s+z_{c\_Bus})} \tag{27}$$

$$\begin{aligned} G_{i_{Bus\_SC}\_i_{busP}}(s) &= Z_{op}(s)G_{vBuspoc}(s)C_{Bus}s \\ &= \frac{z_{c\_Bus}s}{(s+z_{c\_SC})(s+z_{c\_Bus})} \end{aligned} \tag{28}$$

$$\begin{aligned} G_{i_{Bus\_Bat}\_i_{busP}}(s) &= G_{i_{Bus\_SC}\_i_{busP}}(s)\frac{V_{Bus}}{V_{Bat}}G_{i_{Bat}\_i_{SCP}}(s)\frac{V_{Bat}}{V_{Bus}} \\ &= \frac{z_{c\_SC}z_{c\_Bus}}{(s+z_{c\_SC})(s+z_{c\_Bus})} \end{aligned} \tag{29}$$

Figure 10 gives the frequency response range of the DC bus capacitors, supercapacitors and batteries to the power fluctuation. It can be seen that the batteries absorb the low frequency power fluctuation while supercapacitors provide the high frequency part and the rest power is supplied by DC bus capacitors. Meanwhile, the diving frequencies are decided by the crossover frequencies of the DC bus voltage control loop and supercapacitor voltage control loop. So the HESS can be fully used through proper controller design.

4 Experimental and simulation verification

In this section, a HESS, comprising two supercapacitor converters and two battery converters with parameters as listed in Table 1, is built to demonstrate the advanced performance of the proposed control strategy.

The current sharing effect and droop character of two supercapacitor converters are displayed in Fig. 11. The no-load voltage difference before and after calibration are

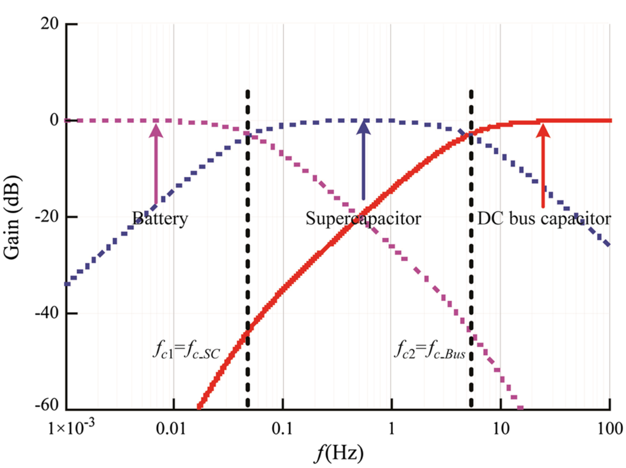

Fig. 10 Response of energy storage to DC bus power fluctuation

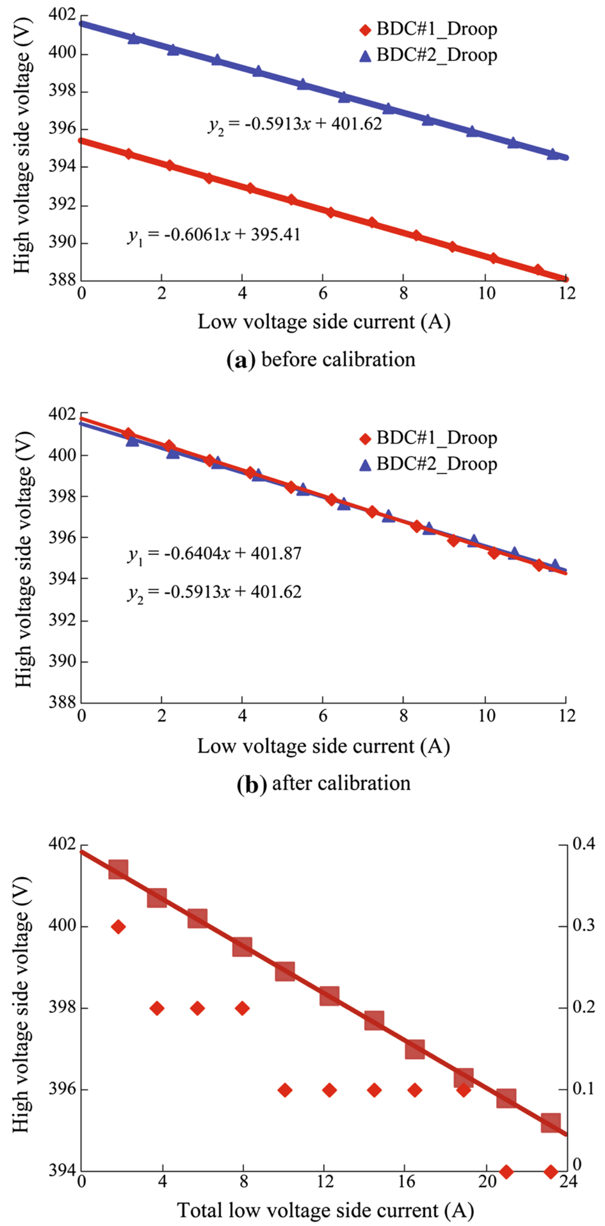

Fig. 11 Current sharing effect

shown in Fig. 11a, b respectively. And the droop curve and current difference are demonstrated in Fig. 11c, which presents a good current sharing result.

The process of SOC balancing and current equalization of batteries is shown in Fig. 12. The initial SOC difference is set to 5% and the measurement of SOC difference is calculated by the Ah-integration as presented in (14). With dual control scheme, the currents of battery units tends to equality and the SOC difference decreases gradually from the initial value 5% to 1.8% in 300 s, which is corresponding to the time constant T_{SOC}.

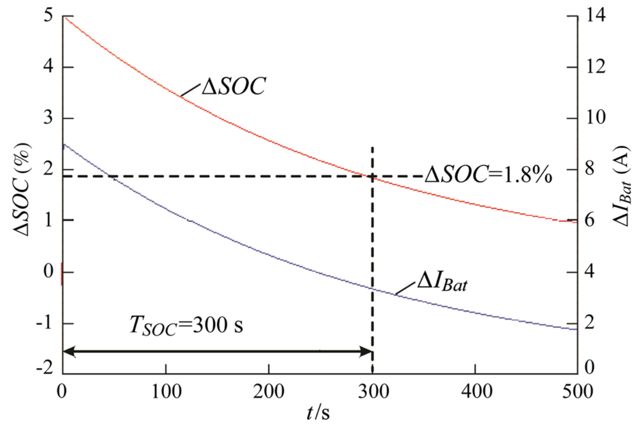

Fig. 12 Results of battery SOC equilibrium and current sharing

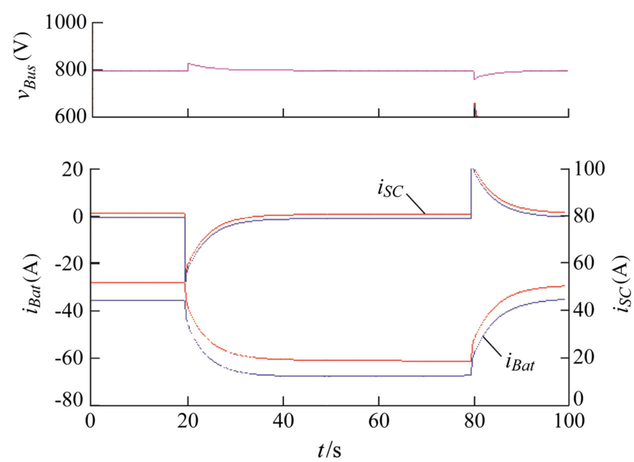

(a) SOC=3%

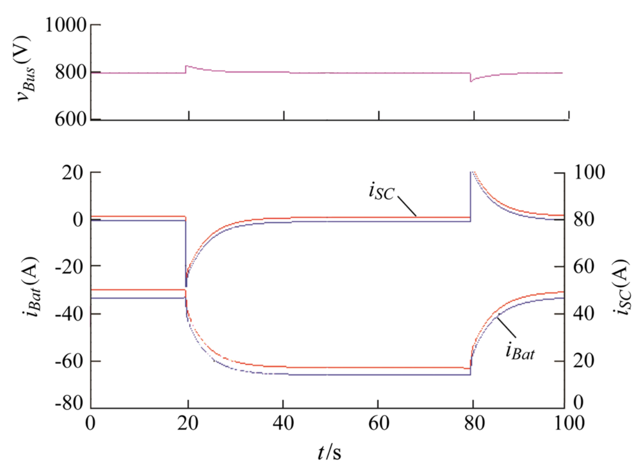

(b) SOC=1.4%

Fig. 13 Dynamic response of supercapacitor and battery current to power fluctuation

Figure 13 shows the dynamic power allocation between supercapacitor and batteries when a 1 kW step load is applied to the system. The supercapacitor responses to the high frequency power fluctuation while the batteries response to the rest power. The output voltage is well regulated at DC bus voltage reference without steady state error since the supercapacitor does not response to the dc component. Meanwhile, it can be seen that the current difference in the case of $\Delta SOC = 3\%$ is larger than that in the case of $\Delta SOC = 1.4\%$. So the current difference is positively correlated to ΔSOC, which helps to SOC equalization.

5 Conclusion

This paper proposes a dual droop-frequency diving coordinated control strategy for HESS in electric vehicle application. The dynamic power allocation is realized through the voltage cascaded control, where the DC bus voltage control loop and supercapacitor voltage control loop set the frequency range for both supercapacitor and battery, make the most use of hybrid energy storage system. On the other aspect, the dual droop control scheme provides not only current sharing between battery units but also SOC equalization without the necessity of communication, which helps to lengthen the battery cycle life and increase the system reliability and flexibility. The experimental results have proven it to be a viable solution for energy management of HESS.

References

[1] Cao J, Emadi A (2012) A new battery/ultracapacitor hybrid energy storage system for electric, hybrid, and plug-in hybrid electric vehicles. IEEE Trans Power Electron 27(1):122–132
[2] Napoli AD, Crescimbini F, Capponi FG et al (2002) Control strategy for multiple input DC-DC power converters devoted to hybrid vehicle propulsion systems. In: Proceedings of the 2002 IEEE international symposium on industrial electronics, L'Aquila, 8–11 July 2002, pp 1036–1041
[3] Zhang SQ, Mishra Y, Ledwich G et al (2013) The operating schedule for battery energy storage companies in electricity market. J Mod Power Syst Clean Energy 1(3):275–284
[4] Venet LP, Guermazi A, Troudi A (2013) Battery/supercapacitors combination in uninterruptible power supply (UPS). IEEE Trans Power Electron 28(4):1509–1522
[5] Zandi M, Payman A, Martin JP et al (2011) Energy management of a fuel cell/supercapacitor/battery power source for electric vehicular applications. IEEE Trans Veh Technol 60(2):433–443
[6] Mendis N, Muttaqi KM, Perera S (2014) Management of battery-supercapacitor hybrid energy storage and synchronous

condenser for isolated operation of PMSG based variable-speed wind turbine generating systems. IEEE Trans Smart Grid 5(2):944–953
[7] Wang L, Li H (2010) Maximum fuel economy-oriented power management design for a fuel cell vehicle using battery and ultracapacitor. IEEE Trans Ind Appl 46(3):1011–1020
[8] Thounthong P, Pierfederici S, Martin JP et al (2010) Modeling and control of fuel cell/supercapacitor hybrid source based on differential flatness control. IEEE Trans Veh Technol 59(6):2700–2710
[9] Camara MB, Dakyo B, Gualous H (2012) Polynomial control method of DC/DC converters for DC-Bus voltage and currents management—battery and supercapacitors. IEEE Trans Power Electron 27(3):1455–1467
[10] Lukic SM, Wirasingha SG, Rodriguez F et al (2006) Power management of an ultra-capacitor/battery hybrid energy storage system in an HEV. In: Proceedings of the 2006 IEEE vehicle power and propulsion conference, Windsor, 6–8 Sep 2006, pp 1–6
[11] Jiang W, Fahimi B (2010) Active current sharing and source management in fuel cell-battery hybrid power system. IEEE Trans Ind Electron 57(2):752–761
[12] Wang GS, Ciobotaru M, Agelidis VG (2013) Power management of hybrid energy storage system for a MW photovoltaic system. In: Proceedings of the 2013 IEEE industrial electronics society Conference, Vienna, 10–13 Nov 2013, pp 6777–6782
[13] Mendis N, Muttaqi KM, Perera S (2014) Management of low- and high-frequency power components in demand-generation fluctuations of a DFIG-based wind-dominated RAPS system using hybrid energy storage. IEEE Trans Ind Appl 50(3):2558–2568
[14] Zhang Y, Jiang ZH (2009) Dynamic power sharing strategy for active hybrid energy storage systems. In: Proceedings of the 2009 IEEE vehicle power and propulsion conference, Dearborn, Michigan, 7–11 Sep 2009, pp 558–563
[15] Garcia FS, Ferreira AA, Pomilio JA (2009) Control strategy for battery-ultracapacitor hybrid energy storage system. In: Proceedings of the 2009 IEEE applied power electronics conference and exposition, Washington, DC, 15–19 Feb, pp 826–832
[16] Zhou HH, Bhattacharya T, Tran D et al (2011) Composite energy storage system involving battery and ultracapacitor with dynamic energy management in microgrid applications. IEEE Trans Power Electron 26(3):923–930
[17] Abbey C, Strunz K, Joós G (2009) A knowledge-based approach for control of two-level energy storage for wind energy systems. IEEE Trans Energy Convers 24(4):539–547
[18] Tani A, Camara MB, Dakyo B (2012) Energy management based on frequency approach for hybrid electric vehicle applications: fuel cell/Lithium-battery and ultracapacitors. IEEE Trans Veh Technol 61(8):3375–3386
[19] Schaltz E, Khaligh A, Rasmussen PO (2009) Influence of battery/ultracapacitor energy-storage sizing on battery lifetime in a fuel cell hybrid electric vehicle. IEEE Trans Veh Technol 58(8):3882–3891
[20] Wang GS, Ciobotaru M, Agelidis VG (2014) Power smoothing of large solar pv plant using hybrid energy storage. IEEE Trans Sustain Energy 5(3):834–842
[21] Yoo H, Sul SK, Park Y et al (2008) System integration and power-flow management for a series hybrid electric vehicle using supercapacitors and batterie. IEEE Trans Appl 44(1):108–114
[22] Dragicevic T, Guerrero JM, Vasquez JC et al (2014) Supervisory control of an adaptive-droop regulated DC microgrid with battery management capability. IEEE Trans Power Electron 29(2):695–706
[23] Chen Z, Ding M, Su JH (2011) Modeling and control for large capacity battery energy storage system. In: Proceeding of the 2011 IEEE electric utility deregulation and restructuring and power technologies, Weihai, 6–9 July 2011, pp 1429–1436

Wuhua LI received the B.Sc. and Ph.D. degree in Applied Power Electronics and Electrical Engineering from Zhejiang University, Hangzhou, China, in 2002 and 2008, respectively. From September 2004 to March 2005, he was a Research Intern, and from January 2007 to June 2008, a Research Assistant in GE Global Research Center, Shanghai, China. From July 2008 to April 2010, he joined the College of Electrical Engineering, Zhejiang University as a Post doctor. In May 2010, he became a faculty member at Zhejiang University as a Lecturer. In December 2010, he was promoted as an Associate Professor. Since December 2013, he has been a Full Professor at Zhejiang University. From July 2010 to September 2011, he was a Ryerson University Postdoctoral Fellow with the Department of Electrical and Computer Engineering, Ryerson University, Toronto, ON, Canada. His research interests include high power devices, advanced power converters and system operation optimization for renewable energy based power systems. Dr. Li has published more than 100 peer-reviewed technical papers and holds over 30 issued/pending patents. Due to his excellent teaching and research contributions, Dr. Li received the 2011 TOP TEN Excellent Young Staff Award and the 2012 Distinguished Young Scholar from Zhejiang University, the 2012 Outstanding Young Researcher Award from Zhejiang Province, the 2012 Delta Young Scholar from Delta Environmental & Educational Foundation and the 2012 National Outstanding Young Scholar. He received three Scientific and Technological Achievements Awards from Zhejiang Provincial Government and the State Educational Ministry of China in 2009 and 2011, respectively.

Chi XU was born in Jiangxi, China in 1990. He received the B.S. degrees from the College of Electrical and Electronic Engineering, Huazhong University of Science and Technology, Wuhan, China, in 2012. He is currently working toward the M.S. degree in the College of Electrical Engineering, Zhejiang University. His research interests include advanced power conversion and control for renewable energy systems.

Hongbin YU was born in Hunan, China, in 1987. He received the B.Sc. and M.Sc. degrees from the College of Electrical Engineering, Zhejiang University, Hangzhou, China, in 2010 and 2013. His current research interests include bidirectional dc–dc converter and energy storage system.

Yunjie GU was born in Hebei, China, in 1987. He received the B.Sc. degree from the Department of Electrical Engineering, Zhejiang University, Hangzhou, China, in 2010, where he is currently working toward the Ph.D. degree in electrical engineering. From May 2011 to January 2012, he was a Research Intern at GE Global Research Center, Shanghai, China. From July to September 2013, he was a Student Visitor at Newcastle University, Newcastle upon Tyne, U.K. His research interests include control and networking of power conversion systems.

Xiangning HE received the B.Sc. and M.Sc. degrees from the Nanjing University of Aeronautical and Astronautical, Nanjing, China, in 1982 and 1985, respectively, and the Ph.D. degree from Zhejiang University, Hangzhou, China, in 1989. From 1985 to 1986, he was an Assistant Engineer at the 608 Institute of Aeronautical Industrial General Company, Zhuzhou, China. From 1989 to 1991, he was a Lecturer at Zhejiang University. In 1991, he obtained a Fellowship from the Royal Society of U.K., and conducted research in the Department of Computing and Electrical Engineering, Heriot-

Watt University, Edinburgh, U.K., as a Postdoctoral Research Fellow for two years. In 1994, he joined Zhejiang University as an Associate Professor. Since 1996, he has been a Full Professor in the College of Electrical Engineering, Zhejiang University. He was the Director of the Power Electronics Research Institute and the Head of the Department of Applied Electronics, and he is currently the Vice Dean of the College of Electrical Engineering, Zhejiang University. His research interests are power electronics and their industrial applications. He is the author or coauthor of more than 280 papers and one book "Theory and Applications of Multi-level Converters." He holds 22 patents. Dr. He received the 1989 Excellent Ph.D. Graduate Award, the 1995 Elite Prize Excellence Award, the 1996 Outstanding Young Staff Member Award and 2006 Excellent Staff Award from Zhejiang University for his teaching and research contributions. He received seven Scientific and Technological Achievements Awards from Zhejiang Provincial Government and the State Educational Ministry of China in 1998, 2002, 2009 and 2011 respectively, and six Excellent Paper Awards. He is a Fellow of the IEEE and has been appointed as the IEEE Distinguished Lecturer by the IEEE Power Electronics Society, in 2011. He is also a Fellow of the Institution of Engineering and Technology (formerly IEE), U.K.